2A.4 A FORMAL EVALUATION OF STORM TYPE VERSUS STORM MOTION

José Miranda and Neil I. Fox
University of Missouri, Columbia, Missouri

1. INTRODUCTION

In the field of atmospheric science, storm motion has been a topic defined by a vast amount of research from numerous agencies. However, defining conclusively storm motion by storm type has been one of the least researched topics in the field. Two of the most widely used nowcasting programs in atmospheric science are the Spectral Prognosis (S-PROG: Seed 2003) and Warning Decision and Support System-Version II (WDSS-II: Lakshmanan et al. 2007) intuitively use storm motion to make nowcasts of precipitation and storm intensity. They automatically track storms and extrapolate motion without regard to storm type or environmental situation. These programs can be further enhanced by classifying severe convective storms by type and subsequently forecasting the motion of the storms from this information---along with existing environmental conditions. Other procedures for forecasting storm motion based on storm type exist (e.g. Lindsey and Bunkers 2004 for supercells, Corfidi et al. 1996 for mesoscale convective complexes). These generally use standard-level wind vectors which may not be appropriate in every case (e.g. the 0-6 km wind or the 850-300-mb wind). These wind levels may not always be representative of the surface layer or cloud layer but are convenient for access as long-standing standard atmospheric levels and model products. On the other hand, the rich variety of model output at numerous levels allows the use of more flexible product selection from Rapid Update Cycle (RUC) or Weather Research and Forecasting Model (WRF) output that could be more closely associated to the motion of a particular storm.

Being able to determine whether storm type is a determining factor in storm motion has several practical results. Forecasters can warn the public in specific areas about certain severe weather threats, giving those warned more time to prepare for potential hazards. Second, applications to industry/business are also affected by storm motion, as the livelihood of many occupations are determined by the amount, intensity, and location of rain, hail, tornadoes, and other weather phenomena. Third, storm type forecasts of storm motion can be used to provide another critical measure of uncertainty, as existing environmental conditions can be documented and "databased" to give forecasters a better idea of the growth, decay, merging, or splitting of storms in certain environmental conditions.

Forecasters presently notify the public of severe weather conditions by noting current surface observations and using extrapolations of cell motion through various modes of radar imagery. By knowing which conditions are conducive to certain types of storms, forecasters will be aided in determining the future motion of those storms, and thus, give a better forecast of severe weather conditions for a given area.

In this study we examine the use of 0°C, -10°C, and -20°C level winds from the RUC-20 as indicators of storm motion. The hypothesis is that choosing winds based on isothermal heights, rather than pressure or surface referenced heights, provides information that is storm relative and more consistent from event to event. Furthermore, the objectives of this study are to determine the pre-existing meteorological conditions associated with three different types of severe convective storm systems (supercell, linear, multi-cell), determine if the statistical classifier can delineate these types based on said meteorological conditions, and finally, determine if storm motion can be more accurately predicted by the success of the statistical classifier in correctly indicating the convective mode of storms at storm genesis.

2. METHODOLOGY

Storm motion can be affected by several factors such as the relative timeframe of the storm in its life cycle, splitting, merging, propagation into stable or unstable air masses, and the relative location of the cell in the parent storm system. For this study, storm motion will be measured in meteorological coordinates (0° indicates from the north, 90° indicates from the east, etc.) unless otherwise stated. This study will attempt to determine if storm motion can be more accurately predicted by classifying storm type and knowing the meteorological conditions associated with those types.

Three different geographical regions of the United States exist as the area of focus for this study. Eighteen (18) storm systems are contained in the three regions classified as eastern, Midwestern, and southern. The eastern region contains cases in the states of Pennsylvania (PA) and Virginia (VA). The Midwestern region contains cases from Missouri (MO), Kansas (KS) and Nebraska (NE), while the southern region contains cases from Tennessee (TN), Texas (TX), Georgia (GA), Mississippi (MS), and Florida (FL). Three regions are

*Corresponding author address: José Miranda, 302 ABNR Building, Univ. of Missouri, Dept. of Soil, Environmental, and Atmospheric Science, Columbia, MO, 65211; email: jmz52@mizzou.edu

used to apply information learned in the study to different sections of the country. The eighteen cases are broken down into three categories defined by the convective mode of storms in the cases: supercell, linear, and multi-cell. Within the events, ambient wind profiles/conditions are noted, and individual cells are identified and tracked for motion.

The first category of case studies consisted of events with supercell characteristics, in which a selection procedure needed to be utilized. Storm cells in this category were picked based on their size. The statistical classifier used in the study allowed a user-defined threshold for the objects, in which supercells smaller than 500km^2 (Lack 2007) in any case were discarded.

Storm cells within this category were also selected based on a user-defined threshold of reflectivity, similar to the Pinto *et al*. (2007) peak reflectivity threshold of 50 dBZ. If the cell on four consecutive scans (~20 min) maintained a peak reflectivity of higher than 50 dBZ, it was included in the study. The use of four scans was determined based on a modified Bunkers *et al*. (2006) definition for two reasons: first, most supercells last shorter than 2 hours; some supercells (rarely) last less than 10 minutes, and, four scans also implies that storm tracking is possible and, above all else, reliable.

The second category of case studies consisted of events with squall-line characteristics, in which individual convective cells within the squall-line were tracked for motion as well as the squall-line itself. Squall-lines in the category were selected based on the Bluestein and Jain (1985) definition of related or similar echoes that form a pattern exhibiting a length-to-width ratio of at least 5:1, greater than or equal to 50 km long, and persisting for longer than 15 minutes (or 3 volume scans). These features were chosen because of they are considered to be mesoscale, as well as their increased probability of containing cells with life cycles relevant to the study as described above.

The third category of case studies consisted of events with multi-cell characteristics, in which cells at different points in their life cycles are tracked for motion. Multi-cells in this category were selected based on their life cycle of less than 1 hour as described by Fovell and Tan (1997) and their user-defined size (roughly 50-100 km^2). Cells in this category were also selected based on a user-defined threshold of reflectivity greater than 30 dBZ as most thunderstorms with multi-cell characteristics rarely produce heavy rainfall (in excess of 50 dBZ) for more than 15 minutes. If the cell maintained a peak reflectivity greater than 30 dBZ for more than 3 consecutive volume scans, it was included in the study.

Radar data for each case were collected from the National Climate and Data Center (NCDC) in the form of level II NEXRAD data and processed through WDSS-II. WDSS-II utilizes a National Severe Storms Laboratory (NSSL) algorithm similar to Johnson *et al*. (1998) which identifies an individual storm's location, movement, and other characteristics within a cell table.

Storm environment data were collected from the NCDC in the form of Rapid Update Cycle-252 (RUC-252) 20 km resolution data for twelve of the eighteen cases. Boundaries were to match the radar Cartesian 256 X 256 km grid, allowing the model data for each case to be overlaid on grids of radar reflectivity.

To track cells for motion and speed a number of steps had to be completed. Radar data were analyzed from the following National Weather Service (NWS) radar sites (Fig. 1): Kansas City, MO (EAX), Memphis, TN (NQA), Amarillo, TX (AMA), Saint Louis, MO (LSX), Hastings, NE (UEX), Atlanta, GA (FFC), Nashville, TN (OHX), Fort Worth, TX (FWS), Jackson, MS (JAN), Tampa Bay, FL (TBW), State College, PA (CCX), Sterling, VA (LWX), and Columbus Air Force Base, MS (GWX).

Figure 1: Radar site locations (thirteen sites) for the eighteen cases in the study. Locations are approximate.

Storm motion and velocity was tabulated for each cell in each case. Both parameters are given by the SCIT algorithm in WDSS-II, while near-storm environments are derived from model data ingested into WDSS-II (similar to Fig. 2). From the model data several parameters were tabulated for each cell. These included height of 0, -10, and -20°C isotherms; mean wind speed from surface to 6 kilometers (measured in knots); storm motion (direction measured in degrees, speed measured in knots); shear from 0-6 kilometers (measured in m s^{-1} km^{-1}); propagation (left or right in the case of supercells and multicells, and direction in the linear cases); mean-layer convective available potential energy (MLCAPE; measured in J kg^{-1}), 0-3-km storm relative helicity (SRH; measured in m^{2}s^{-2}), the u and v-wind components at the 0, -10, and -20°C isotherms (measured in knots), and the Vorticity Generation Parameter (VGP), which is defined in Rasmussen and Blanchard (1998) as

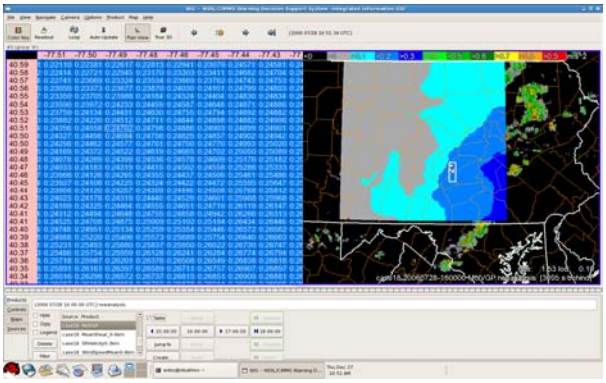

Figure 2: Analyzing RUC-20 Vorticity Generation Parameter Data in WDSS-II.

$$VGP = S(CAPE)^{1/2} \quad (1)$$

where S is the mean shear in the column. These parameters were chosen from the Marwitz (1972) multicell study and the Lack (2007) cell classification study for their usefulness for all storm types. Comparisons of the parameters were then made between cases and similarities/differences were noted.

The cases were subsequently analyzed with a cell identification script in MATLAB with the previous parameter information included. The script also produces images of each convective system for easy reference. With these calculations, the success of the classifier in identifying convective systems of different types was analyzed.

The 0, -10, and -20°C isotherms, as well as their u and v-wind components, were chosen because of their proximity to the cloud layer steering winds (Marwitz 1972) as well as their variability in height in different cases, and subsequent, lack of upper and lower height boundaries. The mean wind speed from the surface to 6 kilometers was chosen as a parameter to compare with the speed of propagation of the individual convective system. The shear from 0-6 kilometers was chosen to note pre-existing environmental conditions prior to storm genesis and to note trends among storms of different types. Propagation, MLCAPE, 0-3 kilometer SRH, and VGP were noted for the same reason.

3. CASE STUDIES

Storm events were divided into three different categories: supercell, squall-line, and multi-cell. The basis for the categories was the appearance of the storms and the orientation of the storm systems (discrete, linear, or clustered). Twelve of the 18 cases had cells that were classified statistically from near-storm environmental data. The other six were used for quality control. This section will outline the statistically analyzed cases.

3.1 12 March 2006: Pleasant Hill, MO region

The National Weather Service (NWS) WSR-88D radar located in Pleasant Hill, MO recorded a supercell event of the period 1900 UTC 12 March 2006 to 2230 UTC 12 March 2006. Two supercells are of note in this event: the first being the "five-state" supercell, which tracked across northeastern Oklahoma, Kansas, Missouri, Illinois, and northwestern Indiana before finally dissipating 17.5 hr after genesis. The second supercell formed just to the north of the five state supercell and eventually merged with it near the Missouri-Illinois border. Figure 3 shows four distinct supercells moving northeast through Missouri on 12 March 2006 that produced several tornadoes.

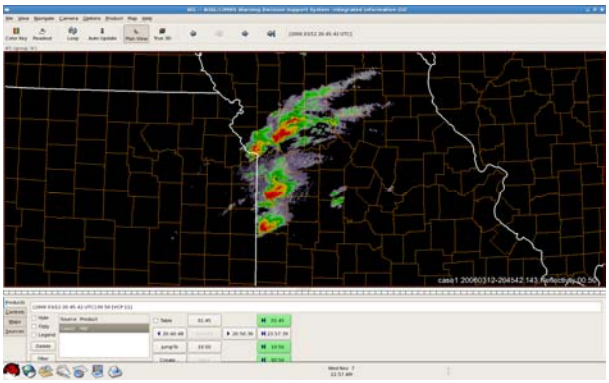

Figure 3: A radar composite reflectivity image from the National Weather Service EAX radar site at 2045 UTC on 12 March 2006. The "five-state" supercell is the cell furthest to the south in the image, along the Kansas/Missouri border.

3.2 2-3 April 2006: Memphis, TN region

This event occurred over two separate regions on 2 April 2006 as discrete supercells merged and formed a squall line stretched from western Illinois south through eastern and southeastern Missouri. In this case, a discrete supercell on the southwestern flank of the squall line was responsible for an F2 tornado that hit the town of Caruthersville, MO, just to the west of the NQA radar site (around 2350 UTC 2 April 2006). This study will focus on the period of 2130 UTC 2 April to 0200 UTC 3 April.

3.3 21-22 April 2007: Amarillo, TX region

An upper level low pressure system which moved out of the intermountain west into the Great Plains was

responsible for this event which occurred near Amarillo, TX from 2200 UTC 21 April 2007 to 0300 UTC 22 April 2007. Numerous supercells on the southwestern flank of an east-moving squall-line are portrayed on the AMA radar image (see figure 4). Maturing over the city, the supercells produced several reports of property damage.

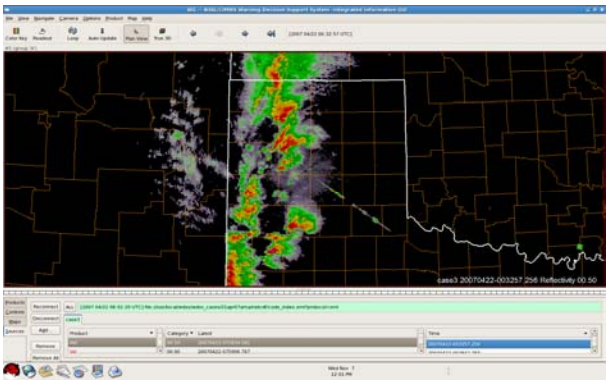

Figure 4: A radar composite reflectivity image from the National Weather Service AMA radar site at 0032 UTC on 22 April 2007.

3.4 28-29 March 2007: Amarillo, TX region

The AMA radar located in Amarillo, TX recorded a left-moving supercell of note from 2100 UTC 28 March 2007 to 0330 UTC 29 March 2007. The storm relative motion of the supercell was north-northwest; it generated from another supercell which was moving to the northeast. The left-moving supercell, however, proved to be much weaker than the parent supercell which produced numerous tornado reports in the panhandle of Texas.

3.5 7 April 2006: Memphis, TN region

The NQA radar site (Memphis, TN) recorded several supercells which moved over the same area over a seven-hour period during the day (1430 UTC to 2130 UTC) of 7 April 2006. As a result, severe flooding affected areas in central Tennessee, with numerous reports of tornadoes as the storms tracked east-northeast. The existence of the cells over the same region for several hours served as a catalyst for flash-flooding.

3.6 19-20 July 2006: Saint Louis, MO region

The NWS WSR-88D radar located in St. Louis, MO (LSX) recorded a southerly moving squall-line (or derecho) that tracked directly the metropolitan St. Louis area from 2230 UTC on 19 July to 0230 UTC 20 July 2006. The region at the time experienced unseasonable warmth, with highs near 100°F with dewpoints at or above 70°F. The squall-line initiated well to the north as an MCS near the Minnesota Iowa border before traveling clockwise with the 500-mb flow into the St. Louis area at 0045 UTC 20 July 2006. Figure 5 shows the easily seen derecho moving through the Saint Louis metropolitan area.

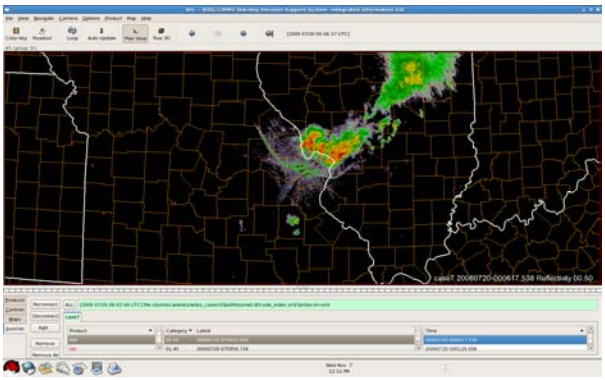

Figure 5: A radar composite reflectivity image from the National Weather Service LSX radar site at 0006 UTC on 20 July 2006.

3.7 21 July 2006: Saint Louis, MO region

The LSX radar site recorded another squall-line with many of the same characteristics as case 4.2.1 roughly 48 hours later (1330 UTC 21 July 2006 to 1730 UTC 21 July 2006) in the St. Louis metropolitan area. The squall-line associated with this case moved from west to east across the area in accordance with the orientation of a stationary front through the region.

3.8 6 November 2005: Saint Charles, MO region

The LSX radar recorded the last squall-line event in this study from 0000 UTC to 0530 UTC 6 November 2005 as an unusually strong low-pressure system tracked across the lower Great Lakes. The northeast to southwest oriented squall-line formed quickly as discrete supercells merged over central Missouri. The squall-line tracked to the east (with individual cells moving northeast along the line) producing numerous reports of hail and wind damage.

3.9 6-7 August 2005: Fort Worth, TX region

The NWS WSR-88D radar site located in Fort Worth, TX (FWS) recorded a multi-cell event from 1830 UTC 6 August 2005 to 0030 UTC 7 August 2005 as daytime instability made the environment favorable for intense vertical motion, and therefore, thunderstorms.

Since wind speeds at all levels were weak, multi-cell thunderstorms were the main type of thunderstorm mode. Figure 6 shows generating and collapsing cells to the west and east of the Fort Worth radar site. Since the cells moved very slowly, the risk for flash flooding was enhanced.

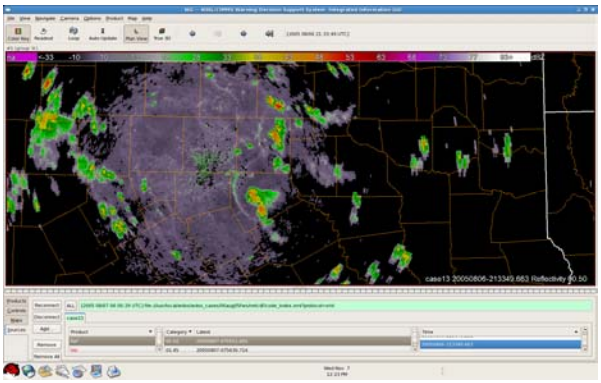

Figure 6: A radar composite reflectivity image from the National Weather Service FWS radar site at 2133 UTC on 6 August 2005.

3.10 19-20 June 2006: Jackson, MS region

The 19-20 June 2006 multi-cell event occurred from 1800 UTC 19 June 2006 to 0000 UTC 20 June 2006 in the Jackson, MS region and DGX radar site. The event propagated across the western side of the radar area as multi-cell thunderstorms formed across central Mississippi and moved west into central Louisiana. Outflow boundaries are a significant contribution to the event as they initiated the genesis of the storms.

3.11 2 July 2006: Tampa Bay, FL region

The mid-summer sea breeze was responsible for these storms as they moved into the Tampa Bay, Florida region and radar site (TBW). The storms moved from east to west (with the surface-925 mb flow) along an outflow boundary easily noticed on radar imagery from 1500 UTC to 2300 UTC. Some of the stronger storms in the case produced hail just to the north of the Tampa Bay metropolitan area.

3.12 28 July 2006: State College, PA region

The fourth case of this type occurred in the State College, Pennsylvania region and CTP radar site as a cold front moved from west to east across the region. Multi-cellular storms formed in central Pennsylvania and moved to the east along the front from 1530 UTC to 2030 UTC, staying discrete as they moved though much of eastern Pennsylvania.

Table 1 shows all 18 cases used in the study.

Date	Radar Site	Abbr.	Storm Type
12-Mar-2006	Kansas City, MO	EAX	Supercell
02-Apr-2006	Memphis, TN	NQA	Supercell
28-Mar-2007	Amarillo, TX	AMA	Supercell
21-Apr 2007	Amarillo, TX	AMA	Supercell
04-May 2003	Topeka, KS	TOP	Supercell
07-Apr-2006	Memphis, TN	NQA	Supercell
19-Jul-2006	Saint Louis, MO	LSX	Linear
21-Jul-2006	Saint Louis, MO	LSX	Linear
9-Jul-2004	Hastings, NE	UEX	Linear
2-May-2003	Atlanta, GA	FFC	Linear
19-Oct-2004	Nashville, TN	OHX	Linear
6-Nov-2005	Saint Louis, MO	LSX	Linear
6-Aug-2005	Fort Worth, TX	FWS	Multicell
19-Jun-2006	Jackson, MS	JAN	Multicell
2-Jul-2006	Tampa Bay, FL	TBW	Multicell
28-Jul-2006	State College, PA	CCX	Multicell
5-Jul-2004	Washington, DC	LWX	Multicell
13-Jun-2004	Memphis, TN	NQA	Multicell

Table 1: Cases used in the study.

4. RESULTS

Figure 7 shows a comparison between actual storm motion and wind direction (in degrees) at the -20°C isotherm for 24 cells tracked in the supercell cases. It can be seen that most of the values lie close to the y=x line (storm motion = winds at the -20°C isotherm).

As stated previously, there are 24 data points in Figure 7. The most, six, are from the April 7, 2006 case in Memphis, while five are from the March 12, 2006 case in Pleasant Hill and the April 21, 2007 case in Amarillo. Four are from the April 2, 2006 case in Memphis and the March 28, 2007 case in Amarillo. On average, results show the actual storm motion to be only 2.7 degrees to the left of the -20°C isothermal wind direction with a standard deviation of 11.8 degrees. A correlation coefficient of 0.91 was found between the -20°C isothermal wind direction and the actual storm motion. These results demonstrate the usefulness of the -20°C isothermal wind in predicting supercell motion. Mean squared error for the values was 141.5.

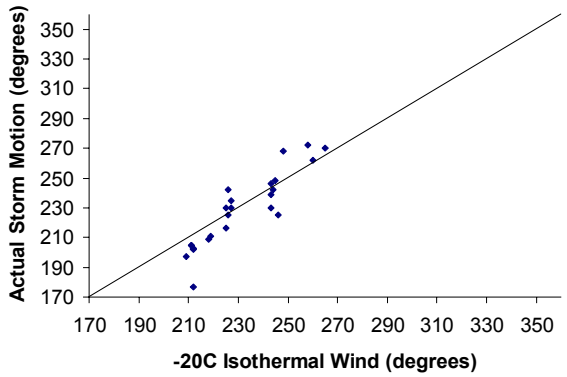

Figure 7: C**omparison between the Actual Storm Motion (degrees) and -20°C isothermal wind (degrees) for cells tracked in supercell cases. The solid line is a line of equality.**

Figure 8 shows a comparison of actual storm motion and wind direction at the -10°C isotherm for the 14 cells tracked in the linear cases. Once again, most of the values lie nowhere close to the y=x trendline. On average, actual storm motion is 25.1 degrees to the right of the -10°C isothermal wind direction with a standard deviation of 45.5 degrees. A correlation coefficient of 0.97 was found, which had a higher amount of predictability than the -20°C isothermal wind/linear storm motion correlation coefficient. Mean squared error for the values was 858.64. The high correlation coefficient shows that most of the error is a result of a bias in the direction which could be easily accounted for.

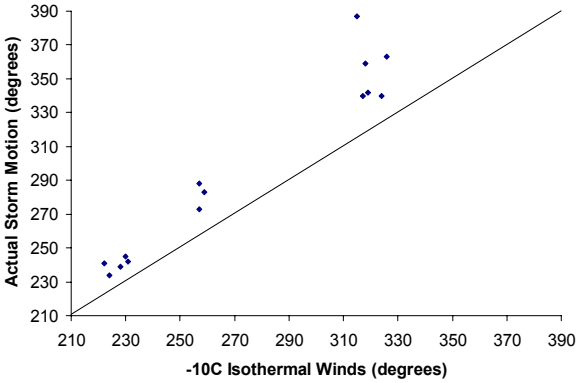

Figure 8: Comparison between the Actual Storm Motion (degrees) and -10°C isothermal wind (degrees) for cells tracked in linear cases. The solid line is a trendline of equality. Values over 360 degrees are cell motions near the 0/360 degree direction discriminator, with 360 degrees added for continuity.

Figure 9 shows a comparison between the actual storm motion of the 15 multicells and the 0°C isothermal wind direction. This comparison had the best correlation coefficient of the three isothermal wind direstions tested for multicells, at 0.37. The average storm motion was 9.1 degrees to the left of the 0°C isothermal wind direction with a standard deviation of 95.6 degrees. Mean squared error for the values was 8620.80. The increased success of the lower-level isotherm in predicting multicell motion backed the hypothesis stated earlier, as eight of the fifteen cells' motions were within 31 degrees of the 0°C isothermal wind direction.

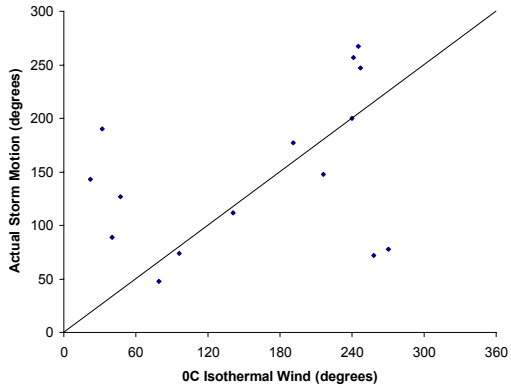

Figure 9: Comparison between the Actual Storm Motion (degrees) and 0°C isothermal wind (degrees) for cells tracked in multicell cases. The solid line is a trendline of equality.

Table 2 is a summary of linear correlation coefficients for each isothermal wind compared to actual cell motion for supercell, linear, and multicell storm systems.

	Supercell	Linear	Multicell
-20°C	0.91	0.95	0.29
-10°C	0.89	0.97	0.11
0°C	0.88	0.97	0.37

Table 2: Linear correlation coefficients for the cells (n = 53) tested in the study as compared to isothermal wind direction.

Table 3 is a comparison of the linear correlation coefficient, standard deviation, and mean squared error for the Isothermal Wind Method versus the LB04 method. The 24 supercells tested in the study were tracked using the LB04 method and compared to the Isothermal Wind Method. The Isothermal Wind Method had the same linear correlation as LBO4, with a larger standard deviation and smaller mean squared error.

Supercells	R	σ	MSE
-20°C Isothermal Wind	0.91	11.8	141.5
LB04	0.91	10.7	150.9

Table 3: Comparison of the linear correlation coefficient, standard deviation (in degrees), and mean squared error (in degrees) for the Isothermal Wind Method as opposed to the LB04 0-6 kilometer mean-wind method.

Table 4 is a comparison of the same statistical parameters for the Isothermal Wind Method versus the C96 method. As with the supercells, the 14 linear cells tested in the study were tracked using the C96 method. The Isothermal Wind method again had the same linear correlation as C96, with a smaller standard deviation and mean squared error.

Linear Systems	R	σ	MSE
-10°C Isothermal Wind	0.97	16.0	858.6
C96	0.97	16.6	876.4

Table 4: Comparison of the linear correlation coefficient, standard deviation (in degrees), and mean squared error (in degrees) for the Isothermal Wind Method as opposed to the C96 mean 850-300 mb wind method.

Table 5 is the comparison of the Isothermal Wind Method versus the M72 method. The 15 multicells in the study after tested by the Isothermal Wind Method were tracked again using the M72 method. The Isothermal Wind Method had a higher linear correlation, with a smaller standard deviation and mean squared error.

Multicells	R	σ	MSE
0°C Isothermal Wind	0.37	95.6	8620.8
M72	0.29	119.8	13694.5

Table 5: Comparison of the linear correlation coefficient, standard deviation (in degrees), and mean squared error (in degrees) for the Isothermal Wind Method as opposed to the M72 0-10 km mean wind method.

The methods outlined for predicting multicell motion had a lower level of success than other methods. On the other hand, predictability remained high no matter what the method in the instance of linear and supercell cases. This may be a function of the particular case, or it may be a case of error within the SCIT cell-tracking algorithm, especially where storms are dominated by ambient low-level winds. If this is the case, however, one can "toggle" the Isothermal Wind Method at lower (higher) isotherms to obtain low (high)-level wind components.

The 53 cells in the study were also tested for similarities in their speed versus the speed of the -20, -10, and 0°C isothermal wind. With supercells, 23 of the 24 cells tested moved slower than the -20°C isothermal wind speed, with the 24th exactly at the -20°C isothermal wind speed. With linear cells, 7 of the 14 moved faster than the -10°C isothermal wind speed, 1 moved at the -10°C wind speed, while 6 moved slower than the -10°C isothermal wind speed. Lastly, with multicells, 12 of the 15 moved faster than the 0°C isothermal wind speed, while the other 3 moved slower. As one moves lower in the atmosphere, the more likely the cell will move faster than the isothermal wind at that level.

5. STORM TYPE CLASSIFICATION

In order to create a dataset for classification, the cells in the study had to be subjectively identified prior to running the classifier. The initial dataset consists of 12 different dates from 2006-2007 with 53 cells individual identified cells covering various geographical regions with the majority in the Midwest and South. As in Lack (2007), the cases span different seasons so the classifier would identify storm type independent of time of year and that cases only deal with warm-season precipitation.

Three different classification types were used in the study and are summarized in Table 6.

Classification Type	Description
Pulse Thunderstorm (Multicell)	Low Shear, CAPE, VGP, SRH
Severe QLCS (Linear)	Medium Shear, SRH; Sig. CAPE, VGP
Supercell	Sig. Shear, SRH; Medium CAPE, VGP

Table 6: The three classification types used within the classification tree study.

Once the storms were individually identified, a table was generated with all storm attributes and tagged with one of the three categories. This information was used to determine the best use of parameters to determine cell type. The results are classified as a "tree" with nodes at each branch with represents the best "split" of the data (Lack 2007). The result is a deterministic solution that labels the cell in a certain class. For information on the classification tree scheme, consult Lack (2007), Breiman *et al.* (1984), or Burrows (2007).

Figure 7 shows the classification tree derived from the information obtained of the 53 cells in the study. The first split using a 0-6 kilometer wind shear value of 58.45 kts results in a separation of multicell or pulse thunderstorms (low shear) from severe linear cells and supercells (high speed and/or directional shear), resulting in a correct analysis of all 15 multicells in the study.

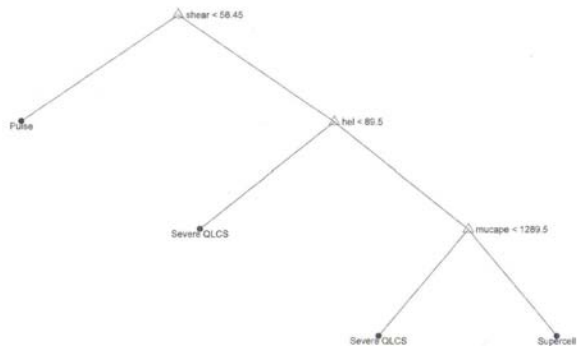

Figure 7: Cell classification tree for the 53 cells in the study.

The second split using a 0-3 kilometer storm relative helicity value of 89.5 m^2 s^{-2} separates linear cells with helicities less than 89.5 m^2 s^{-2} from linear cells with helicities greater than 89.5 m^2 s^{-2} or supercells. This split separated weakly rotating from strongly rotating storms and resulted in a correct analysis of 22 of the 24 supercells used in the study. The third and last split of the tree using a MLCAPE value of 1289.5 J kg^{-1} designated cells with helicities greater than 89.5 m^2 s^{-2} and MLCAPE values of less than 1289.5 J kg^{-1} as linear cells with the rest being supercells. This resulted in a correct classification of 9 of the 14 linear cells. One reason for the drop in accuracy is the severity of the linear cases and the large MLCAPE and SRH values for some of the linear cells, which ultimately were not classified correctly. The tree which was created with uneven populations of storms satisfied the hypothesis proposed by Lack (2007) in which smaller-scale storms are classified more accurately as the population becomes more uneven. Of the 53 cells, 46 were classified correctly.

6. CONCLUSIONS

Examining data among the three types of cells in the study showed a strong correlation between the -20°C isothermal wind and supercell motion. A significant correlation between the 0°C isotherm and multicell motion was also noted. Cell tracking by isothermal wind direction also performed with a higher level of predictability than previous studies. Lastly, many of the cells used in the study were correctly identified by the statistical classifier using near-storm environmental model data. Knowing the convective mode of storms at genesis helps the forecaster to make a deterministic evaluation of storm motion, velocity, severity, and duration in a given area. Thus, finding a correlation between storm type and storm motion gives forecasters the chance to make more accurate forecasts of storm type and where the storms will have an effect.

The results of the study in applying near-storm environment model data to the cells identified are summarized in the following points:

- Supercell thunderstorms tend to move with the -20°C isothermal wind direction; have the highest variability in 0-6 kilometer wind shear; and move slower than the -20°C isothermal wind speed.
- Cells in linear systems were found to move with the -10°C and -20°C isothermal wind direction; have the highest variability in mean layer CAPE, 0-3 kilometer storm relative helicity, and the vorticity generation parameter; and have no propensity to move slower or faster than the -10°C isothermal wind speed.
- Multicell thunderstorms have a marginal linear correlation to the 0°C isothermal wind direction; typically have the lowest CAPE, shear, VGP, and SRH values; and move faster than the 0°C isothermal wind speed.

The results of the study in applying classification tree techniques are summarized forthwith:

- Cell classification with smaller non-rotating storms was more accurate; the discriminators used to separate types of storms made intuitive sense.
- Discriminating between cells in linear systems and supercells using the MLCAPE parameter resulted in a less than desirable success rate; the use of VGP is a more successful parameter to use as documented by Lack (2007) and other previous studies.
- Hybrid cases, as theorized by Lack (2007), seem to decrease the success rate of the statistical classifier; more research is needed in the area to evaluate the significance of this claim.
- Additional storm attributes may be needed to more successfully classify types of storms.

As discussed earlier, the primary goal of evaluating storm type versus storm motion is to give forecasters a better chance of telling the public the potential dangers of a given type of storm in a forecast area. Classification can be used in real-time by forecasters to monitor particularly severe storms, or to make a historical archive of storms for different inter-annual time frames. As explained in Lack (2007), the primary goal of the classification tree scheme is to use the information given by the model data to input into nowcasting products for cell morphology purposes.

The research obtained in this study first notes that different pre-existing meteorological conditions exist for supercell, linear, and multicell systems. Second, the classification tree system successfully classified different storm types in most cases. The understanding of storm morphology and the addition of storm type, if

not included or even neglected in a nowcast, may mean severe conditions can be underestimated, missed, or even ignored.

Future work for the evaluation of storm type versus storm motion includes the accounting and solving of several errors. Such errors as small sample size, hybrid cases, separating parameters, selection of isotherms, calculation of parameters, and data assimilation are the foundation for future work to be conducted on this topic.

In order to obtain the ideal-sized tree, a dataset with hundreds or perhaps even thousands of cells from hundreds of cases are needed. This leads to future research of perhaps an automated system of classifying and a historical archive of thousands of cells for study. Being able to consult the historical archive for research would lead to more consistent results with storm motion and cell classification. Hybrid cases in future work could solely be used for a separate study; this would effectively evaluate the usefulness of the classifier in delineating cells of different types on an intra-case basis. Future work to the tree classification system can include parameters of azimuthal shear, as well as parameters derived from dual-polarization radar (Lack 2007). A study of merging or splitting cells may also be needed to update the classifier with those cells that may have different physical characteristics than others used in this study.

Other research that can be conducted in the future may be to divide the linear cases into the divisions made by Bluestein and Jain (1985). This allows researchers to determine the properties of back-building cells and embedded-areal cells. This may lead to an explanation of the severity of linear cells in the cases in this study. The selection of isotherms closer or further from the surface may give nowcasters a better correlation between isothermal wind and linear/multicell systems. Lastly, the improvement of nowcasting products with increased automation will give forecasters a chance to use the data gathered in real-time, and subsequently, forecast for storm severity or hazardous weather conditions with higher levels of accuracy and timeliness.

The addition of the future work stated above, along with the research presented in this study will be more useful for a more accurate forecast of storm motion by storm type.

7. REFERENCES

Bluestein, H.B., and M.H. Jain, 1985: Formation of mesoscale lines of precipitation: severe squall lines in Oklahoma during the spring. *J. Atmos. Sci.,* 42, 1711-1732.

Breiman, L., J.H. Friedman, R.A. Olshen, and C.J. Stone, 1984: Classification and Regression Trees. Chapman and Hall, pp. 358.

Bunkers, M.J., B.A. Klimowski, J.W. Zeitler, R.L. Thompson, and M.L. Weisman, 2000: Predicting supercell motion using a new hodograph technique. *Wea. Forecasting,* 15, 61-79.

Burrows, W.R., 2007: Dynamical-statistical models for lightning prediction to 48-hr over Canada and the United States. *Preprints: 5th Conference on Artificial Intelligence Applications to Environmental Science, San Antonio, TX.*

Corfidi, S.F., J.H. Merritt, and J.M. Fritsch, 1996: Predicting the movement of mesoscale convective complexes. *Wea. Forecasting,* **11,** 41-46.

Fovell, R.G., and P.-H. Tan, 1996: Why multicell storms oscillate. Preprints, *18th Conf. Severe Local Storms,* San Francisco, CA, *Amer. Met. Soc.,* 186-189.

Johnson, J.T., P.L. Mackeen, A. Witt, E.D. Mitchell, G.J. Stumpf, M.D. Elits, and K.W. Thomas, 1998: The Storm Cell Identification and Tracking Algorithm: An Enhanced WSR-88D Algorithm. *Wea. Forecasting,* **13,** 263-276.

Lack, S.A., 2007: Cell identification, verification, and classification using shape analysis techniques. D.Phil. dissertation, Dept. of Soil, Environmental, and Atmospheric Sciences, University of Missouri, 147 pp.

Lakshmanan, V., T. Smith, G. J. Stumpf, and K. Hondl, 2007: The warning decision support system – integrated information (WDSS-II). *Wea. Forecasting*, **22** (3), 596-612.

Lindsey, D.T., and M.J. Bunkers, 2004: Observations of a severe, left-moving supercell on 4 May 2003. *Wea. Forecasting,* **20,** 15-22.

Marwitz, J.D., 1972a: The structure and motion of severe hailstorms. Part II: multicell storms. *J. Appl. Meteor.,* **11,** 180-188.

Pinto, J., C. Kessinger, B. Hendrickson, D. Megenhardt, P. Harasti, Q. Xu, P. Zhang, Q. Zhao, M. Frost, J. Cook, and S. Potts, 2007: Storm characterization and short term forecasting using a phased array radar. *33rd Conference on Radar Meteorology,* Cairns, Queensland, Australia.

Seed, A. W., 2003: A dynamic and spatial scaling approach to advection forecasting. *J. Appl. Meteorol.*, **42** (3), 381-388.